Proceedings of 2004 IEEE/RSJ International Conference on
Intelligent Robots and Systems
September 28 - October 2, 2004, Sendai, Japan

A Virtual Prosthetic Hand Using EMG Signals for fMRI Measurements

Yoshiyuki TANAKA[1)] Satoshi NODA[2)] Toshio TSUJI[1)]

Masaharu MARUISHI[3)] Osamu FUKUDA[4)]

1) Graduate School of Eng., Hiroshima Univ., Higashi-hiroshima, JAPAN, {ytanaka, tsuji}@bsys.hiroshima-u.ac.jp
2) Sanyo Electric Co., Ltd., Osaka, JAPAN, s-noda@rd.sanyo.co.jp
3) Hiroshima Prefectural Rehabilitation Center, Higashi-hiroshima, JAPAN, maruishi@rehab-hiroshima.gr.jp
4) National Institute of Advanced Industrial Science and Technology, Tsukuba, JAPAN, fukuda.o@aist.go.jp

Abstract— **This paper proposes a virtual EMG-prosthetic hand system using a neural network available in an fMRI room. A subject attaches surface electrodes on his forearm, and manipulates the virtual EMG-prosthetic hand visualized with 3D computer graphics by using visual biofeedback projected on a screen in the scan room. The preliminary experiments demonstrate that the intended hand motion by the subject can be determined with high discrimination rates over 96 % without decaying fMRI images. Finally, in order to show the validity of the proposed system, we report the neurological experiments that were carried out to analyze human brain functions.**

I. Introduction

It has been increased the number of people amputated their upper extremities by labor accident, traffic accident, or a land mine in the world. Most of such amputees equip a cosmetic prosthetic hand or an internally powered prosthesis, while an externally powered prosthesis using electric motors is seldom employed mainly because of three aspects; no financial public support for purchasing, the insufficient performance of its hardware, and the inexperienced skill of an amputee in operating such electric-driven prosthesis. So far, many efforts have been paid to develop an intelligent prosthetic hand with much higher functions by using electromyographic (EMG) signals, but less attention to design an effective training method for an amputee to become skilled in the use of such intelligent prosthesis.

There have been a few studies on a training method for operating an EMG prosthetic hand. For example, Dupont and Morin proposed a training system for manipulating the powered prosthetic hand by using computer graphics [1], in which a trainee can control a virtual hand created by computer graphics according to his muscle contraction level. However the training motions in their system are only hand open and close. There exists an assistant tool for an EMG prosthetic hand that can suggest the suitable positions to attach electrodes and the amplification factor in measuring EMG signals [2]. However it is difficult to apply into the training because the available information is too small. Then, Tsuji et al. constructed a training system which advices much intelligible visual information for the functional recovery of muscle activation control needed in manipulating an EMG prosthetic hand [3]. They also reported that the amputee could obtain the sensation that he manipulated the prosthetic hand as his own hand in the progress of the training with the developed system. This suggests that some brain functions of a trainee may be changed by the training effect. If the skill level of operating the prosthesis can be evaluated from brain functional activations, it can be utilized as an effective index for the training and also as the basic data for developing a novel training methodology.

On the other hand, magnetic resonance imaging (MRI) has been the primary technique for the diagnosis and treatment of neurological disorders, and provides detailed images of the interior of human brain structures that may not be visualized with other imaging methods [4]. The MRI can observe the change of blood volume in different area of a human brain with high spatial resolution, and it is called *functional MRI* (functional magnetic resonance imaging: fMRI) [5]. A number of studies have been carried out to analyze brain functions by using fMRI [6]–[8]. For example, Flament et al. reported that the activation area of a brain is gradually straitened as the training goes on under the visual-motor task using a joystick [6]. However, these researches focusing on motor control function did not discuss the quantitative relationship between functional activations of a human brain and biological signals, such as EMG, electrocardiogram (ECG) and so on, during a motor task, mainly because there does not exist a measuring system of such a biological signal available in the fMRI environment. As a result, there has been no research on functional activations of a brain in manipulation of an EMG prosthetic hand.

In this paper, as a first step for the quantitative analysis of human brain activations accoridng to the skill level in manipulating an EMG prosthetic hand, a virtual EMG prosthetic hand available in fMRI measurements is developed.

II. EMG measurements in an MRI equipment

Since the MRI uses radio waves and strong magnetic field with high tesla for acquiring fMRI images, tremen-

0-7803-8463-6/04/$20.00 ©2004 IEEE

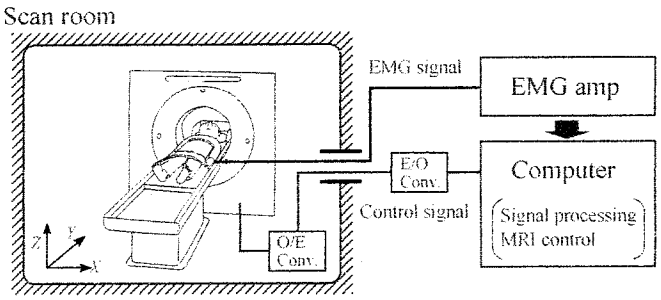

Fig. 1. The overview of an EMG measuring system

dous strong noise signals are induced in the measured EMG signals. This section describes an EMG measuring system available in the fMRI that can discard such induced noise signals in detail.

A. Configuration of an EMG measuring system

Figure 1 illustrates an overview of the developed measuring system of EMG signals in fMRI measurements. An EMG measuring instrument as well as a computer for signal processing and MRI control is set at the outside of the scan room, because such instruments made of magnetic matters cause a mechanical failure of the MRI and a serious medical accident.

The EMG signals measured from surface electrodes are transmitted to an EMG amplifier (NIHON KOHDEN, MEM-4204) by signal cables through the waveguide as shown in Fig. 1, and are amplified 500 times after filtering out with the band-pass filter (cut-off frequency: 10 [Hz] for the lower and 500 [Hz] for the upper). The amplified signals are then inputted into a computer by an A/D converter (sampling frequency: 1.0 [kHz]; quantization: 12 [bits]).

The computer controls the scanning timing of fMRI images by transmitting the trigger signal toward the MRI equipment (MAGNETOM SYMPHONY: SIEMENS, the static magnetic field strength: 1.5 [T]; the gradient magnetic field strength: 34 [mT/m]; the type of magnet: superconductivity) via an electric-optical converter without inducing external noises into the scan room, so that the start time of measuring EMG signals and fMRI images can be synchronized in the experiment.

B. Discarding nosed EMG signals in fMRI

Figure 2 shows an example of EMG signals during the wrist flexion measured at the outside and inside of the scan room, in which a pair of electrodes was attached to extensor carpi ulnaris of the subject (male, Age 23). The EMG signal in the figure (b) was recorded with the developed measuring system during fMRI measurements. As shown in Fig. 2(b), the remarkable noise signals are observed in the EMG signal. It is thus required to remove such noise signals from EMG signals for the functional analysis of a human brain in a motor task with fMRI images.

Such noise signals are induced by the change of gradient magnetic field and radio wave for acquiring each tomographic image of a brain, and the time of changes depends

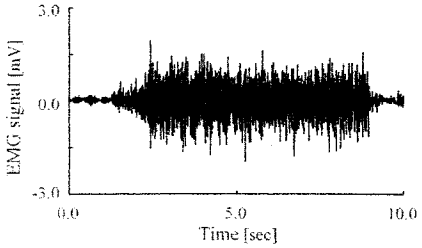

(a) EMG-signal in the normal environment

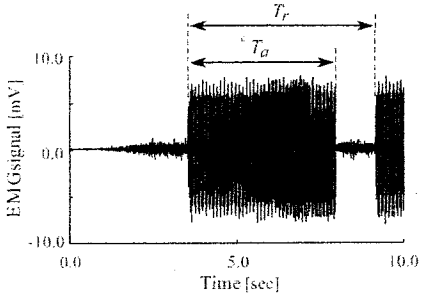

(b) Noised EMG-signal in the fMRI measurement

Fig. 2. Examples of the measured EMG signals in fMRI

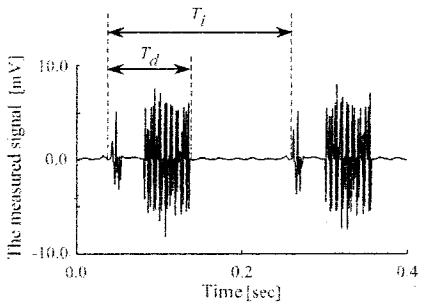

Fig. 3. Noise signals with respect to the fMRI sequence parameters

on the number of tomographic images for acquiring the three-dimensional image of a whole brain (S_n), the time for acquiring a set of S_n images (T_a), and the time between repetitions of the sequence (T_r). Then, the time interval for acquiring each fMRI image (T_i) can be settled by $T_i = T_a/S_n$.

Here, the developed system can manage the repetition time T_r to match the starting time of measuring EMG signals and fMRI images by sending the trigger signal to the MRI equipment. Therefore, it is possible to control the time period of generating noise signals on EMG signals by regulating the three sequence parameters in fMRI measurements, ie., T_r, T_a and S_n. Paradoxically, it can be much expected to obtain a meaningful EMG signal by discarding noised EMG signals signal in fMRI measurements based on the relationship between the noise signal and the sequence parameters.

Figure 3 shows the measured EMG signals in the scan room under the sequence parameters were set as T_r = 11 [s], T_a = 8.8 [s] and S_n = 40. It can be seen that T_i is almost agreed with the calculated time 220 [ms]. It should be noted that the noise signals are induced only during

the time period T_d (about 110 [ms]). This indicates that an EMG signal can be measured without affected by the scanning of fMRI images during the time period $(T_i - T_d)$.

C. Measuring experiment of EMG signals

The EMG signals were measured with a subject (male, Age 23) in which four pairs of electrodes were attached to four muscles in his right arm (Ch 1: extensor carpi ulnaris, Ch 2: flexor carpi ulnaris, Ch 3 and Ch 4: flexor carpi radialis). In the experiment, the subject was asked to extend his wrist joint from 5.0 [s] to 10.0 [s] according to the voice instruction from the interphone.

Figure 4 shows an example of the experimental results under the same sequence parameters in Fig. 3 with $T_d = 130$ [ms]. The figure (a) is the EMG signals measured at the outside of the scan room; the figure (b) and (c) represent at the inside of the scan room during fMRI measurements without and with the proposed algorithm for noised signals, respectively. Muscle contraction cannot be observed from the EMG signals in the figure (b) because of the heavy noise arose from the changes of radio wave and gradient magnetic field. On the other hand, it can be seen that the amplitude and motion pattern of EMG signals by the proposed algorithm (Fig. 4(c)) are almost agreed with those at the outside of scan room (Fig. 4(a)).

From the above experimental results, it can be confirmed that a meaningful EMG signal can be measured by utilizing the fMRI sequence parameters although the frequency information of the EMG signal is lost as a result of discarding the noised signal measured during the time period T_d.

III. Virtual EMG-based prosthetic hand system for MRI environments

Figure 5 shows an overview of the developed virtual EMG prosthetic hand control system in this paper. This system estimates an operator's intended motion from the de-noised EMG signals explained in the previous section by using a neural network, and presents smooth hand motions similar to those of the human hand by means of the impedance control method. The following subsections describe each part of the proposed virtual hand system in detail.

A. Feature extraction of the EMG signals

First, the EMG signals measured from L pairs of electrodes are processed to gauge the meaningful EMG signals by means of the proposed algorithm explained in II-B for manipulating the virtual prosthetic hand. The de-noised EMG signals are then rectified and filtered out through a second order Butterworth filter (cut-off frequency: 1 [Hz]) in which a zero-order hold is applied in the time period of removing noise signals.

The processed EMG signals $EMG_l(t)$ $(l = 1, \cdots, L)$ are normalized with the sum of L channels by

$$x_l(t) = \frac{EMG_l(t) - EMG_l^{st}}{\sum_{l'=1}^{L}(EMG_{l'}(t) - EMG_{l'}^{st})}, \quad (l = 1, \cdots, L) \tag{1}$$

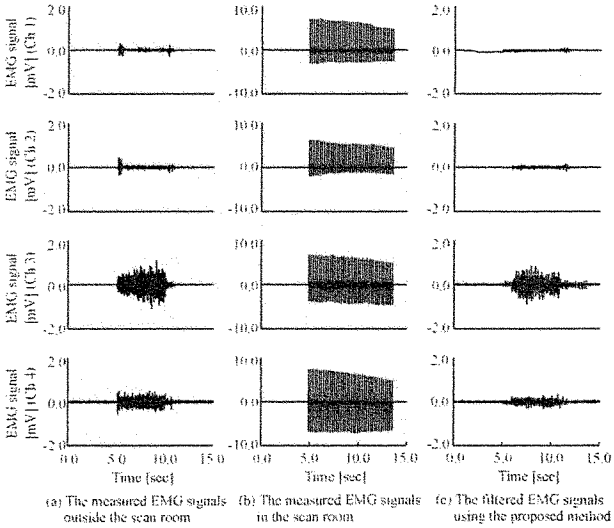

Fig. 4. Isolation of the induced noise signal from the EMG signals using the proposed method

where EMG_l^{st} is a mean value of $EMG_l(t)$ measured in the rest condition. An EMG pattern for each hand movements of an operator can be represented by the vector $\boldsymbol{x}(t) = [x_1(t), x_2(t), \cdots, x_L(t)]^{\mathrm{T}} \in \Re^L$.

B. Pattern classification of hand motions

In this paper, a log-linearized Gaussian mixture network (LLGMN) [9] is utilized as a neural network to estimate the intended hand motion of an operator, which can provide high discrimination performance of a biological signal that much changes depending on individuals, physical fatigue, perspiration, and so on.

The input of the LLGMN $\boldsymbol{X}(t) \in \Re^H$ is created with the vector $\boldsymbol{x}(t) \in \Re^L$ as follows:

$$\begin{aligned}\boldsymbol{X}(t) = [&1, \boldsymbol{x}(t)^{\mathrm{T}}, x_1(t)^2, x_1(t)x_2(t), \cdots, \\ &x_1(t)x_L(t), x_2(t)^2, x_2(t)x_3(t), \\ &\cdots, x_2(t)x_L(t), \cdots, x_L(t)^2]^{\mathrm{T}}.\end{aligned} \tag{2}$$

The first layer consists of H $(H = 1 + L(L+3)/2)$ units corresponding to the dimension of $\boldsymbol{X}(t)$, and the identity function is used for an activation function of each unit.

Each unit $\{c, m\}$ $(c = 1, \cdots, C;\ m = 1, \cdots, M_c)$ in the second layer receives the output ${}^{(1)}O_h(t)$ of the first layer weighted by the coefficient $w_h^{(c,m)}$. The relationship between the input ${}^{(2)}I_{c,m}(t)$ and the output ${}^{(2)}O_{c,m}(t)$ in the second layer is given by

$${}^{(2)}I_{c,m}(t) = \sum_{h=1}^{H} {}^{(1)}O_h(t) w_h^{(c,m)}, \tag{3}$$

$${}^{(2)}O_{c,m}(t) = \frac{\exp[{}^{(2)}I_{c,m}(t)]}{\sum_{c'=1}^{C}\sum_{m'=1}^{M_{c'}} \exp[{}^{(2)}I_{c',m'}(t)]}, \tag{4}$$

where $w_h^{(C,M_C)} = 0$ $(h = 1, 2, \cdots, H)$, C and M_c denote the number of classes and the number of components belongs to class c.

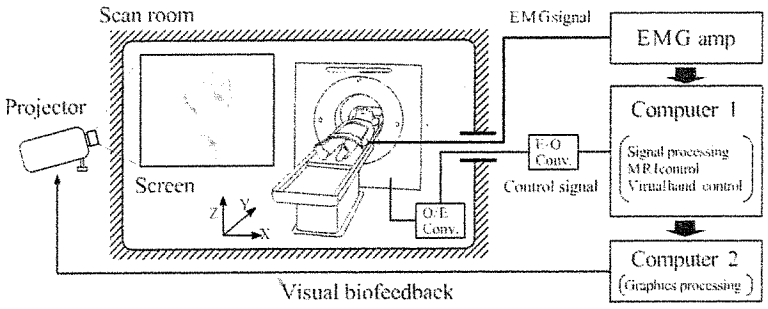

Fig. 5. The overview of an EMG measuring system

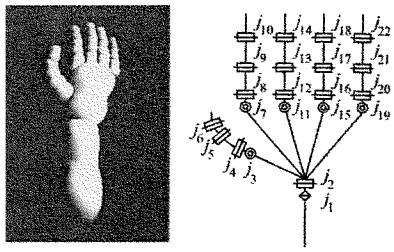

Fig. 6. A link model of the virtual prosthetic hand

The unit c in the third layer integrates the outputs of M_c units in the second layer, and the relationship between the input ${}^{(3)}I_c(t)$ and the output ${}^{(3)}O_c(t)$ is described as

$$ {}^{(3)}I_c(t) = \sum_{m=1}^{M_c} {}^{(2)}O_{c,m}(t), \tag{5} $$

$$ Y_c(t) = {}^{(3)}I_c(t). \tag{6} $$

The output of the third layer $Y_c(t)$ correspond to *a posteriori* probability of the class c for the inputted EMG pattern $\boldsymbol{x}(t)$.

The LLGMN is trained via a supervised learning with a teacher vector $\boldsymbol{T}^{(t)} = (T_1^{(t)}, \cdots, T_c^{(t)}, \cdots, T_C^{(t)})^{\mathrm{T}}$ for the input vector $\boldsymbol{x}(t)$ that created from the actual hand motion measured in the preliminary experiment, where $T_c^{(t)} = 1$ for the particular class c while $T_c^{(t)} = 0$ for all the other classes. The learning of the LLGMN is performed to maximize the likelihood via minimization of the following energy function J as

$$ J = \sum_{t=1}^{T} J_t = -\sum_{t=1}^{T}\sum_{c=1}^{C} T_c^{(t)} \log Y^c(t), \tag{7} $$

in which the learning rule is designed with the concept of terminal attractor (TA) [10] so that the convergence time of the function can be specified.

C. Motion discrimination of the virtual hand

The discrimination of hand motions is conducted according to the entropy of LLGMN's outputs and the force information to recognize whether the motion has really occurred or not.

The entropy indicates, or may be interpreted as, a risk of ill-discrimination [11], and it can be calculated with the outputs of the LLGMN, *a posteriori* probability of each motion c, as

$$ H(t) = \frac{-\sum_{c=1}^{C} Y^c(t) \log_2 Y^c(t)}{\log_2 C}, \tag{8} $$

where large entropy means that the output of the LLGMN is ambiguous.

Then, the force information $F_{EMG}(t)$ is calculated in order to decide the beginning of hand movements by

$$ F_{EMG}(t) = \frac{1}{L}\sum_{l=1}^{L}(EMG_l(t) - EMG_l^{st}). \tag{9} $$

TABLE I

IMPEDANCE PARAMETERS IN THE VIRTUAL HAND CONTROL

Joint, j	Motion	m_j	$b_{j,1}$	$b_{j,2}$	$b_{j,3}$	$k_{j,1}$	$k_{j,2}$	$k_{j,3}$
1	Pronation / Supination	0.004	0.34	0.2	0.144	32.0	0.69	3.2
2	Extention / Flexion	0.003	0.34	0.2	0.144	32.0	0.60	2.7
3 ~ 6, 8 ~ 10, 12 ~ 14, 16 ~ 18, 20 ~ 22	Hand grasping / opening	0.002	0.09	0.2	0.040	0.9	0.60	0.3
7, 11, 15, 19	Hand grasping / opening	0.002	0.70	0.2	0.040	1.9	0.60	0.3

The determination is suspended when the entropy is over the specified threshold H_d defined beforehand. While the Bayes decision rule is utilized to determine a specific class under the entropy is less than H_d. The final decision for controlling the virtual hand motion is performed only in the case that the force information $F_{EMG}(t)$ is over the normal threshold F_d which is the calculated value beforehand when the hand motion is appeared.

D. Biomimetic impedance control of the virtual hand

The virtual prosthetic hand has 22 joints as shown in Fig. 6, and its motion of each joint is impedance-controlled with the human hand impedance properties on the basis of the determination result and the force information $F_{EMG}(t)$ so that a operator can manipulate the virtual hand naturally as if he moves his own hand.

The dynamics of the j-th joint of the virtual hand is written by

$$ I_j\ddot{\theta}_j + B_j(\alpha_j)\dot{\theta}_j + K_j(\alpha_j)(\theta_j - \theta_j^o) = \tau_j - \tau_j^{ex}, \tag{10} $$

$$ \tau_j(t) = \alpha_j(t)\tau_{jc}^{max}, \tag{11} $$

where α_j denotes the muscular contraction ratio for the j-th joint motion; I_j, $B_j(\alpha_j)$ and $K_j(\alpha_j)$ denote the joint inertia, viscosity and stiffness, respectively; θ_j and θ_j^e are the computed and the equilibrium angles of the j-th join; and τ_j, τ_j^{ex} and τ_{jc}^{max} are the joint torque, the external torque and the prespecified maximum torque in the motion c $(c = 1, \cdots, C)$.

The muscular contraction ratio α_j is calculated by using $F_{EMG}(t)$ as

$$ \alpha_j(t) = \frac{F_{EMG}(t)}{F_c^{max}}, \tag{12} $$

where F_c^{max} is the mean value of F_{EMG} measured in the maximum voluntary contraction (MVC) for the motion c. The joint viscosity and stiffness are modeled with a nonlinear function with respect to α_j as

$$B_j(\alpha_j) = b_{j,1}\alpha^{b_{j,2}} + b_{j,3}, \quad (13)$$

$$K_j(\alpha_j) = k_{j,1}\alpha^{k_{j,2}} + k_{j,3}, \quad (14)$$

where $b_{j,n}$, $k_{j,n}$ (n=1,2,3) are experientially determined with reference to the estimated impedance parameters of human arm as shown in Table I [12].

IV. Experiments

A. Virtual hand operation experiments

The verification of the proposed virtual hand system were carried out with five normal subjects in fMRI measurements, in which the MRI equipment was controlled under the same sequence parameters settled in Fig. 4. In the experiments, a subject was instructed to change his hand motion as open, grasp, extension and flexion ($C = 4$) according to the beep sound from the computer in the order.

Figure 7 shows an example of the experimental results by Subject A, where the four pairs of electrodes were attached to his right forearm (Ch 1: flexor digitorum profundus, Ch 2: flexor pollicis longus, Ch 3: flexor carpi ulnaris, Ch4: Extensor carpi ulnaris). In order from the top of Fig.7, the measured EMG signals during fMRI measurements, the EMG signals by the proposed algorithm of discarding noised signals, the force information $F_{EMG}(t)$, the entropy $H(t)$, and the discrimination results of hand motion are plotted. It can be seen that the hand motions intended by the subject can be successfully estimated from the EMG signals measured during fMRI measurements although the large noise signals are induced.

The discrimination rate of hand motions were 100.0 % for Subject A, 99.9 % for Subject B, 96.7 % for Subject C, 96.2 % for Subject D, and 98.8 % for Subject E.

B. Human brain activations in the virtual hand operation

Finally, human brain functions were investigated with subjects during the motor control task using the developed virtual hand system, in which four pairs of electrodes were attached to the subject's right forearm (Ch 1: extensor carpi ulnaris, Ch 2: flexor carpi ulnaris, Ch 3 and Ch 4: flexor carpi radialis). The fMRI measurements were conducted with the same sequence parameters in Fig. 7 (T_r = 11 [s], S_n = 40, TE = 60 [ms]) by means of the single-shot echo-planar image (EPI) under matrix size: 64 × 64, FOV: 192 [mm], voxel size: 3 × 3 × 3 [mm^3], and the number of the functional volume in each task: 30.

In the analysis of human brain activations using fMRI images, the relevant tasks are carried out along the designed paradigms that have generally several periods of rest alternating with several periods of activation. Therefore, in this paper, two experimental conditions of the motor task, hand open/grasp motion, were prepared by using the developed virtual hand system with the designed paradigms as shown in Fig. 8;

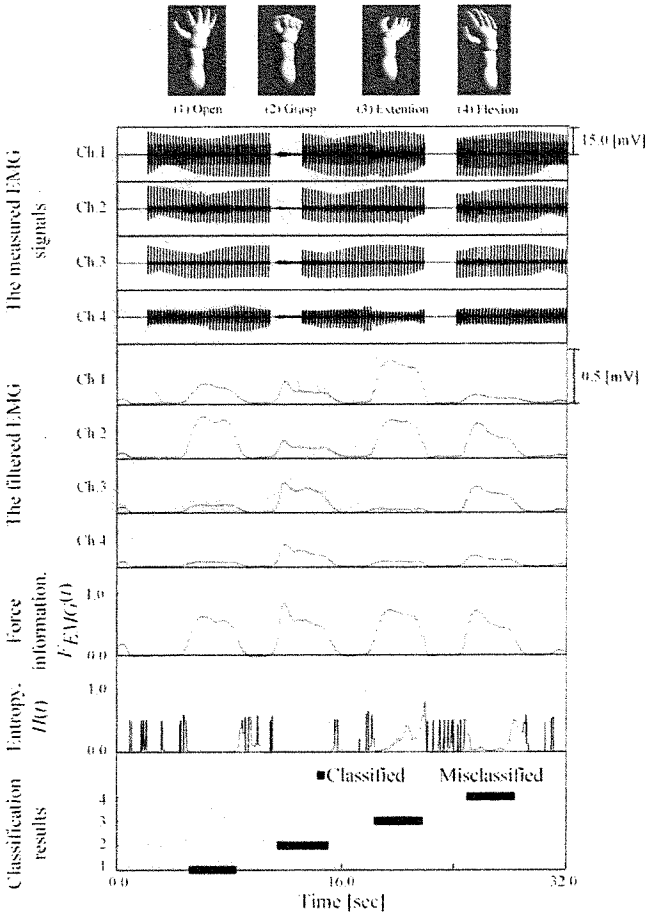

Fig. 7. An example of the virtual hand operation experiments (Subject A)

- Task 1: A subject is instructed to rest and close his/her eyes in the rest period, while perform the hand open/grasp motion in time to the beep sound without opening his eyes in the activation period.
- Task 2: A subject is instructed to rest and close his/her eyes in the rest period, while perform the hand open/grasp motion in time to the beep sound with watching the virtual hand projected on the screen in the activation period.

The beep is regularly sounded with the interval time at 1.1 [s] during fMRI measurements including the rest period to eliminate the influence of auditory stimuli on brain activations for a given motor task in the fMRI image analysis.

The fMRI image processing for identifying functional activations of a human brain was performed by Statistical Parametric Mapping (SPM) [13] with SPM99 implemented in MATLAB 5.3 (Math Works Inc). The acquired fMRI images were regulated on the basis of the first volume by the rigid body transformation and normalized into anatomical standard stereotaxic space with the Montreal Neurological Institute template (MNI) because of the individual differences in the shape of a brain. The normalized images were spatially smoothed by a Gaussian filter (full width at half maximum: 8 [mm]) to remove the other

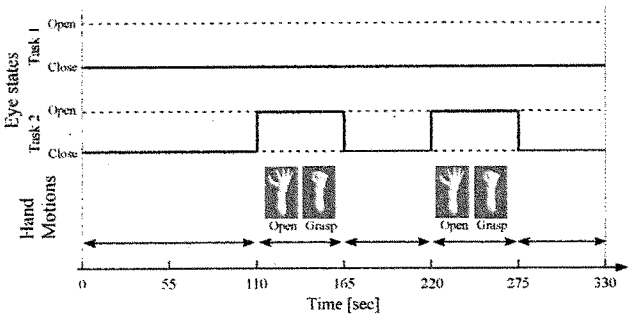

Fig. 8. The fMRI paradigms used in the experiments

individual differences.

Figure 9 shows the examples of brain activation maps for each task, where the warm colors represent functional activation area for the given motor task. It can be seen that primary motor area and sensorimotor cortex activate in both tasks. In addition to these area, bilateral primary visual area, bilateral visual association area, bilateral ventral premotor cortex activate in Task 2. These differences between the brain activation maps of Task 1 and Task 2 represent the brain functions for manipulating the virtual prosthetic hand.

Thus, it can be expected to reveal important brain functions to operate a prosthetic hand via experiments with healthy volunteers using the developed system, and to collect basic data that will be useful to develop a skill training method of manipulating an EMG-prosthetic hand for amputees [14].

V. Conclusions

This paper has proposed a measuring method of EMG signals in fMRI measurements by using the scanning timing of fMRI images. Then, the virtual EMG prosthetic hand system has been constructed for the analysis of human brain activations accoridng to the skill level in manipulating an EMG prosthetic hand. The preliminary experiments with the subjects demonstrated that the intended hand motion of the subject could be determined with high discrimination rates without decaying fMRI images. Finally the neurological experiments using the developed system were carried out to analyze brain functions in operating the virtual hand.

Future study will be directed to improve a signal processing method to isolate noise factors due to the acquisition of fMRI images from the biological signal, and also investigate the differences on brain activation during operation of the virtual hand between a normal subject and an amputee.

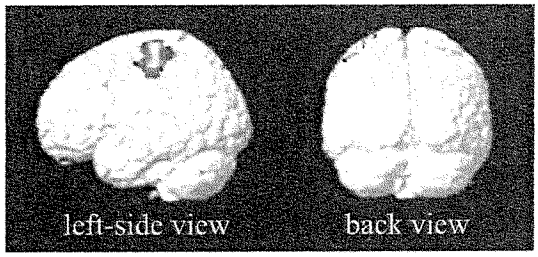

(a) Task 1

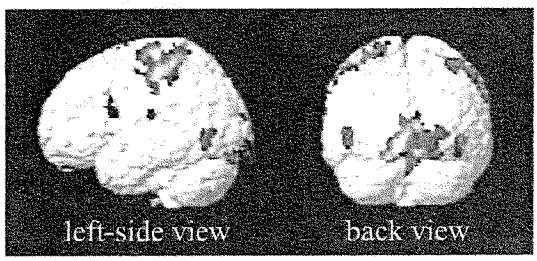

(b) Task 2

Fig. 9. Activation maps of the human brain in operating the virtual hand (Subject B)

References

[1] A. C. Dupont and E. L. Morin: "A Myoelectric Control Evaluation and Trainer System," *IEEE Transactions on Rehabilitation Engineering*, Vol. 2, No. 2, pp. 100–107, 1994.

[2] For example, http://www.p-supply.co.jp

[3] T. Tsuji, O. Fukuda, A. Otsuka, and M. Kaneko: "A Training System for EMG Manipulation of Prosthetic Arms," *The Transactions of the Institute of Electronics, Information and Communication Engineers*, Vol. J83-D-II, No. 10, pp. 2030–2039, 2000 (in Japanese).

[4] T. Nakai, M. Hattori, T. Hiraga, K. Matsuo, K. Kuroda, S. Murakami and T. Moraya: "Evolution of Magnetic Resonance Technologies from NMR to MRI, and toward fMRI; Their Medical Applications," *National Institute of Advanced Industral Science and Technology Bulletin*, Vol. 63, No. 3, pp. 13–28, 1999 (in Japanese).

[5] M. Fukunaga, T. Tanaka, M. Umeda, T. Ebisu, I. Aoki, Y. Someya, Y. Watanabe, Y. Mori and S. Naruse: "functional MRI of Brain," *Japanese Society for Magnetic Resonance in Medicine*, Vol. 21, No. 6, pp. 204–216, 2001 (in Japanese).

[6] D. Flament, J. M. Ellermann, S. G. Kim, K. Ugurbil, T. J. Ebner: "Functional magnetic resonance imaging of cerebellar activation during the learning of a visuomotor dissociation task,"*Human Brain Mapping*, Vol. 4, pp. 210–226, 1996.

[7] T. Takahashi, R. Xiao, M. Inase, K. Kansaku, T. Iijima: "Spatio-temporal activation pattern of fMRI signal after hand movements revealed by averaged single trial method," *NeuroImage*, Vol.7, s937, 1998.

[8] K. Toma , M. Honda, T. Hanakawa, T. Okada, H. Fukuyama, A. Ikeda, S. Nishizawa, J. Konishi, H. Shibasaki: "Activities of the primary and supplementary motor areas increase in preparation and execution of voluntary muscle relaxation: an event-related fMRI study," *The Journal of Neuroscience*, Vol. 19, pp. 3527–3534, 1999.

[9] T. Tsuji, O. Fukuda, H. Ichinobe and M. Kaneko: "A Log-Linearized Gaussian Mixture Network and Its Application to EEG Pattern Classification", *IEEE Transactions on Systems, Man, and Cybernetics-Part C: Applications and Reviews*, Vol. 29, No. 1, pp. 60–72, February, 1999.

[10] M. Zak: "Terminal attractors for addressable memory in neural networks," *Physics Letters A*, Vol. 133, pp. 218–222, 1988.

[11] T. Tsuji, H. Ichinobe, K. Ito and M. Nagamachi: "Discrimination of Forearm Motions from EMG Signals by Error Back Propagation Typed Neural Network Using Entropy," *Transaction of the Society of Instrument and Control Engineers*, Vol. 29, No. 10, pp. 1213–1220, 1993 (in Japanese).

[12] O. Fukuda, T. Tsuji, M. Kaneko and A. Otsuka: "A Human-Assisting Manipulator Teleoperated by EMG Signals and Arm Motions," *IEEE Transactions on Robotics and Automation*, Vol.19, No.2, pp.210–222, April 2003.

[13] Y. Nagahama: "SPM: As Image Processing Soft of Functional MRI," *INNERVISION*, Vol. 14, No. 9, pp. 74-78, 1999 (in Japanese).

[14] M. Maruishi, Y. Tanaka, H. Muranaka, T. Tsuji, Y. Ozawa, S. Imaizumi, M. Miyatani, and J. Kawahara: "Brain activation during manipulation of the myoelectric prosthetic hand: a functional magnetic resonance imaging study," *NeuroImage*, Vol.21, No.4, pp.1604–1611, April 2004.